

## Intersite Coupling Effects in a Kondo Lattice

S. Nakatsuji,<sup>1</sup> S. Yeo,<sup>1</sup> L. Balicas,<sup>1</sup> Z. Fisk,<sup>1</sup> P. Schlottmann,<sup>2</sup> P. G. Pagliuso,<sup>3</sup> N. O. Moreno,<sup>3</sup>  
J. L. Sarrao,<sup>3</sup> and J. D. Thompson<sup>3</sup>

<sup>1</sup>National High Magnetic Field Laboratory (NHMFL), Florida State University, Tallahassee, Florida 32310

<sup>2</sup>Department of Physics, Florida State University, Tallahassee, Florida 32306

<sup>3</sup>Los Alamos National Laboratory, Los Alamos, New Mexico 87545

(Received 23 May 2002; published 14 August 2002)

The La dilution of the Kondo lattice CeCoIn<sub>5</sub> is studied. The scaling laws found for the magnetic susceptibility and the specific heat reveal two well-separated energy scales, corresponding to the single-impurity Kondo temperature  $T_K$  and an intersite spin-liquid temperature  $T^*$ . The Ce-dilute alloy has the expected Fermi liquid ground state, while the specific heat and resistivity in the dense Kondo regime exhibit non-Fermi-liquid behavior, which scales with  $T^*$ . These observations indicate that the screening of the magnetic moments in the lattice involves antiferromagnetic intersite correlations with a larger energy scale in comparison with the Kondo impurity case.

DOI: 10.1103/PhysRevLett.89.106402

PACS numbers: 71.27.+a, 75.20.Hr, 75.30.Mb

The nonuniversal behavior of heavy fermion compounds has challenged experimental and theoretical physicists for many years. A wide range of low-temperature phenomena, such as strongly enhanced paramagnetism, magnetic/quadrupolar long-range order, Kondo insulators, unconventional superconductivity, and non-Fermi-liquid behavior, have been reported. This variety of phenomena is believed to arise through the competition and interplay of the Kondo effect, band structures, and intersite correlations. Both the Kondo-esque resonance at the Fermi level [1] and the Ruderman-Kittel-Kasuya-Yosida (RKKY) interaction in a Kondo lattice are the consequence of the large Coulomb repulsion in the partially filled  $4f(5f)$  shell in conjunction with the hybridization of the  $f$  electrons with the conduction state.

In the single-impurity limit, the low energy transport and the thermodynamic properties scale with a single parameter, the Kondo temperature  $T_K$  [1]. As  $T$  is decreased below  $T_K$ , the moments which are localized at high temperatures are screened into local singlets by the conduction electrons, giving rise to a local Fermi liquid state. The agreement between experiment and theory is excellent for many dilute systems [2].

For Kondo lattice systems, it has been a long-standing issue how the intersite interactions affect the local character of the Kondo screening. If the singlet formation in the lattice involves the neighboring localized moments, it is expected that the spin screening is accompanied by antiferromagnetic (AF) short-range correlations, which may modify  $T_K$  or yield a new energy scale. While a study of the Kondo lattice within the Gutzwiller approximation [3] predicts such a "lattice enhancement" of  $T_K$ ,  $1/N$  expansions [4] indicate local singlet formation with no change in the energy scale. The lattice enhancement has been confirmed by Monte Carlo, exact diagonalization, and density matrix renormalization group [5] for the 1D Kondo lattice, but backscattering across the Fermi surface may affect this result. Monte Carlo studies for the 2D half-filled Kondo

lattice yield different renormalizations of the spin and charge gaps [6].

Experimentally, the strength of the intersite coupling can be varied by substituting the magnetic Ce ions by their nonmagnetic analog La. This approach continuously interpolates between the Kondo lattice and the single-impurity limit. Several systems have been studied, e.g., (Ce, La)Al<sub>2</sub>, (Ce, La)B<sub>6</sub>, and (Ce, La)Cu<sub>6</sub> [7], but it is hard to arrive at quantitative conclusions, since La substitution often changes both the crystalline electric field (CEF) parameters and Kondo coupling.

The ideal conditions of concentration independent  $T_K$  and CEF are met for (Ce, La)Pb<sub>3</sub> [8]. It was reported that the specific heat and susceptibility scale with the Ce concentration for the entire alloying range and follow the predictions of the  $S = 1/2$  Kondo impurity model with  $T_K \simeq 3$  K [8]. No signs of intersite couplings were found, except in the concentrated limit, where they eventually lead to the AF ordering at  $T_N \simeq 1$  K for CePb<sub>3</sub>.

In this Letter we present experimental evidence for three well-separated energy scales in Ce<sub>1-x</sub>La<sub>x</sub>CoIn<sub>5</sub>:  $T_K$ , the energy scale for intersite interactions  $T^*$ , and the level splitting due to CEF. CeCoIn<sub>5</sub> is a heavy fermion unconventional superconductor with a high transition temperature  $T_{sc} = 2.3$  K [9–11]. With La dilution, Ce<sub>1-x</sub>La<sub>x</sub>CoIn<sub>5</sub> has a paramagnetic ground state with Ce keeping essentially the same valence and CEF splitting through the entire alloying range. We found scaling functions with the energy scale  $T^*$  for the deviations of the specific heat and the susceptibility from the single-impurity behavior. This scale  $T^*$  is attributed to intersite interactions. The specific heat in the dense Kondo regime exhibits non-Fermi-liquid behavior with the characteristic temperature  $T^*$ , while for dilute alloys it follows that of the  $S = 1/2$  Kondo impurity model. The deviation of the susceptibility from the single-ion behavior shows a strong decrease below  $T^*$ , suggesting the formation of a spin liquid. The scaling procedure reveals that  $T^*$  systematically increases from

the single-ion  $T_K$  with increasing Ce concentration. This indicates that the screening process of the localized moments in the lattice has higher energy scale, involving AF intersite correlations.

Single crystals were prepared using an In self-flux method [9,12]. Before growing the crystals, Ce and La metals are premixed by arc-melting at least 10 times to get a homogeneous mixture. X-ray powder diffraction patterns show a single phase tetragonal  $\text{HoCoGa}_5$  structure, which can be viewed as alternating layers of  $(\text{Ce, La})\text{In}_3$  with layers of  $\text{CoIn}_2$  along the  $c$  axis. The resistivity was measured by standard four-probe dc and ac techniques down to 25 mK using the low-temperature facilities at the National High Magnetic Field Laboratory. The magnetization was measured down to 1.8 K with a Quantum Design SQUID magnetometer and the specific heat ( $C_P$ ) by a thermal relaxation method.

Figure 1 shows the magnetic part of the in-plane resistivity  $\rho_m$  defined as the difference in  $\rho(T)$  of  $(\text{Ce, La})\text{CoIn}_5$  and  $\text{LaCoIn}_5$  (the nonmagnetic, isostructural, analog of  $\text{CeCoIn}_5$ ) divided by the Ce concentration,  $1-x$ . Above 50 K, the  $\rho_m$  data for all  $x$  collapse onto a single curve with the  $-\log T$  dependence characteristic of the Kondo effect. Hence, the high  $T$  Kondo temperature,  $T_K^h$ , is essentially independent of  $x$ . In the Ce rich region,  $\rho_m$  shows coherent metallic behavior after rising through a peak that defines the coherence temperature  $T_{\text{coh}}$ . The La dilution reduces  $T_{\text{coh}}$ , which tends to zero near  $x = 0.5$ , where  $\rho_m$  saturates below 500 mK. With further La dilution,  $\rho_m$  evolves toward single-ion behavior with a  $\log T$  dependence down to 500 mK that suggests a small  $T_K$  of about 1–2 K. Hence,

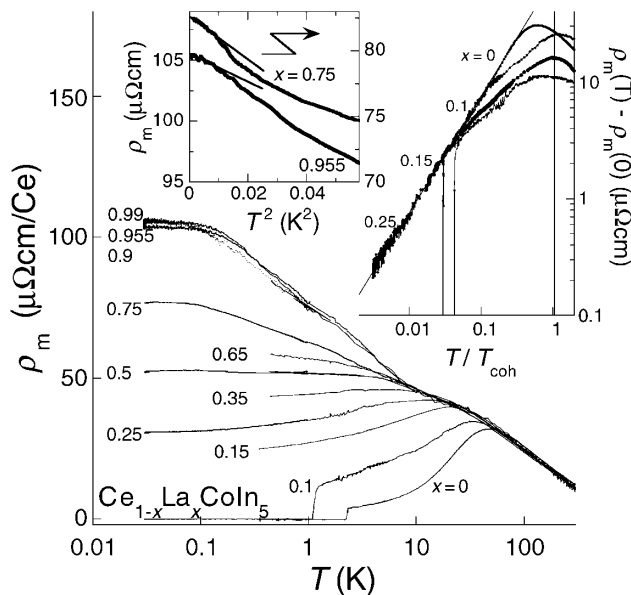


FIG. 1. Magnetic in-plane resistivity  $\rho_m$  for various  $x$  of  $\text{Ce}_{1-x}\text{La}_x\text{CoIn}_5$ . Right inset: The log-log plot for the inelastic part of  $\rho_m$  vs  $T/T_{\text{coh}}$ ; the solid line is the  $T$  linear fit and the vertical lines mark the onset of superconductivity. Left inset:  $\rho_m$  vs  $T^2$  for the incoherent regime.

106402-2

$x = 0.5$  roughly separates the coherent and single-ion regimes. It is interesting to note that 50% is close to the percolation limit of 41% of a 2D square lattice (consistent with the 2D nature of Ce-Ce nearest neighbor network in the  $\text{CeIn}_3$  layers).

The inset of Fig. 2 shows the  $c$ -axis component of the susceptibility  $\chi_c(T)$  per mole Ce vs  $\log T$ . As for  $\rho_m$ , the data above 80 K collapse onto the same curve for all concentrations, again indicating that  $T_K^h$  is independent of  $x$ . The high  $T$  data follows the modified Curie-Weiss law  $\chi(T) = C/(T + \sqrt{2}T_K^h)$  [1] with  $T_K^h \approx 35$  K and an effective paramagnetic moment of  $2.5\mu_B$ . In contrast, at low  $T$ ,  $\chi(T)$  increases with La dilution, reaching the single-impurity limit for  $x \geq 0.95$ . Similar systematics are also observed for the  $ab$ -plane component,  $\chi_{ab}(T)$ .

We performed a CEF fit to the  $ab$ -plane and  $c$ -axis components of the susceptibility for the dilute Ce regime (see solid line in the inset of Fig. 2). The ground state is found to be a  $\Gamma_7^{(1)}$  doublet  $(-0.39| \pm 5/2) + 0.92| \mp 3/2)$ , including a low-temperature Weiss temperature of 2 K) with a fairly large gap to the excited  $\Gamma_7^{(2)}$   $(0.92| \pm 5/2) + 0.39| \mp 3/2)$ ,  $\Delta_1 = 148.0$  K) and  $\Gamma_6$   $(| \pm 1/2)$ ,  $\Delta_2 = 196.5$  K) doublets. This scheme also well fits the high- $T$  susceptibility above 80 K for all  $x$  for both the  $ab$ -plane and  $c$ -axis components, which suggests that the CEF scheme is essentially independent of  $x$ . In order to confirm the CEF scheme, we measured the specific heat up to 200 K for  $x = 0, 0.25, 0.50, 0.75$ , and 1.00. The magnetic contribution to the specific heat  $C_m$  is estimated as  $C_P$  of  $\text{Ce}_{1-x}\text{La}_x\text{CoIn}_5$  minus  $C_P$  of  $\text{LaCoIn}_5$  divided by the Ce concentration. For all  $x$ ,  $C_m$  shows a broad peak around 100 K, consistent with the Schottky-type fit based on the above CEF scheme (see Fig. 3, right inset). These data also imply that the CEF scheme is roughly independent of  $x$ . There are differing CEF fits for  $\text{CeCoIn}_5$  in the literature. Our results agree best with the scheme of Ref. [10] and less well with those

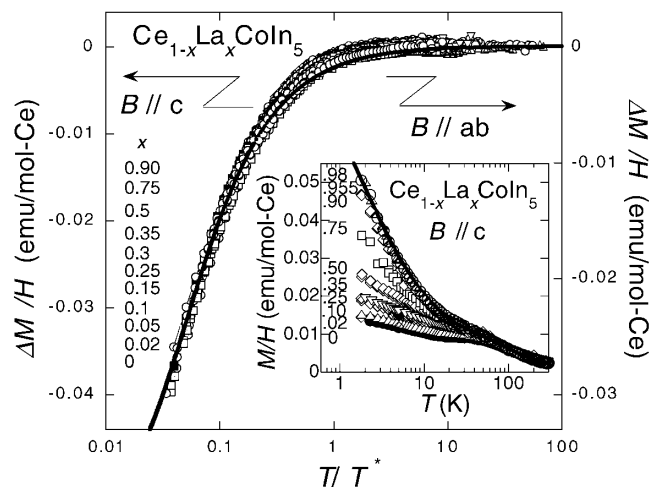


FIG. 2. Excess susceptibility  $\Delta\chi(T) \equiv \chi(T) - \chi_0(T)$  ( $\chi_0(T)$  refers to the single-impurity limit at  $x = 0.955$ ), scaled with  $T/T^*$ . The solid line corresponds to an activation type fit. Inset: the  $c$ -axis component of  $M/H$  vs  $\log T$ .

106402-2

in Ref. [13]. We argue that these discrepancies arise from the way intersite correlations are taken into account.

Given the essential same CEF scheme for all  $x$ , we interpret the change in  $\chi(T)$  with La dilution at low  $T$  as an intersite coupling effect. To quantify this contribution, we subtract the single-impurity CEF  $\chi(T)$  from  $\chi(T)$  for each  $x$  to get the “excess susceptibility”  $\Delta\chi(T)$ , which shows a strong decrease of  $\chi$  at a concentration dependent characteristic temperature  $T^*$  (e.g., around 50 K for CeCoIn<sub>5</sub>). Interestingly, we found a scaling law for both  $ab$  and  $c$  components of  $\Delta\chi(T)$  vs  $T/T^*(x)$ , as shown in Fig. 2. Basically the same systematic change of  $T^*$  with  $x$  is found for both components of  $\chi$ ,  $T^{*ab}$  and  $T^{*c}$ , as seen in Fig. 4.

For Kondo systems  $C_m/T$  is given by  $1/T^{*s}$  ( $T^{*s}$  is a characteristic energy) times a scaling function of  $T/T^{*s}$  [1]. Actually, we have found two different scaling functions in Ce<sub>1-x</sub>La<sub>x</sub>CoIn<sub>5</sub>. In the coherent region ( $x < 0.5$ ), for the temperature range between  $0.04T^{*s}$  and  $0.6T^{*s}$ ,  $C_m/T$  fits well to the expression  $-5.4/T^{*s} \ln(T/T^{*s})$  (J/mol-Ce K<sup>2</sup>) as displayed by the solid line in Fig. 3. Considering that 5.4 J/mol-Ce K is close to  $R \ln 2$ , this expression suggests that  $T^{*s}$  gives the temperature scale to recover the ground doublet entropy. In the incoherent regime ( $x > 0.5$ ), all the curves scale to another function as shown in Fig. 3. Furthermore, the  $C_m/T$  data for  $x = 0.98$  and  $0.99$  agrees well with the exact results for the  $S = 1/2$  single-ion Kondo model with the single parameter  $T_K = 1.7$  K, which defines the  $T^{*s}$  at the single-impurity limit [14] (see left inset of Fig. 3).

Generally,  $T_K$  is related to the high-temperature  $T_K^h$  and the CEF splittings via  $k_B T_K = (k_B T_K^h)^3 / \Delta_1 \Delta_2$  [15]. From the susceptibility we have  $T_K^h \approx 35$  K,  $\Delta_1 = 148$  K, and  $\Delta_2 = 196.5$  K, such that the expression yields  $T_K \approx$

1.5 K, consistent with the  $T^{*s}$  and the low- $T$  Weiss temperature in the single-impurity limit.

With the scaling procedures above, we obtain a systematic La concentration dependence of  $T^{*s}$  as shown in Fig. 4. There are three points to note. First, the characteristic temperatures  $T^{*s}$ ,  $T^{*ab}$ , and  $T^{*c}$  are essentially identical, indicating that there is only one energy scale besides  $T_K$ . Second, in the  $x \rightarrow 1$  limit this energy scale agrees with  $T_K$ , showing that the scale  $T^*$  originates from the single-ion  $T_K$ . Third, in the dense Kondo limit CeCoIn<sub>5</sub>,  $T^*$  coincides with the  $T_{\text{coh}}$  of the resistivity.

Because  $T_K^h$  is constant throughout the alloy series, and the high  $T\chi$  and  $C_p$  data point to no changes in the CEF parameters, the single-ion  $T_K$  should also be constant. *The systematic increase in  $T^*$  must then arise from the intersite coupling.* Hence, this system has three well-separated energy scales:  $T_K \approx 1$ –2 K for the single-ion Kondo screening,  $T^* \approx 40$ –50 K for Kondo lattice effects and the CEF excitations  $\Delta \approx 200$  K. The fact that these energy scales are very different is a fortuitous situation that allows the present scaling analysis.

The different scaling of  $C_m/T$  in the coherent and incoherent regimes suggests that the nature of the ground state changes near  $x = 0.5$ . A qualitative change was also found in the low- $T$  dependence of the resistivity. The right-hand inset of Fig. 1 shows the log-log plot of the inelastic part of the in-plane resistivity vs  $T/T_{\text{coh}}$  in the coherent regime. All curves for  $x \leq 0.25$  have a  $T$ -linear dependence below a characteristic temperature  $T_{\text{linear}}$ . Note that all the  $T$ -linear curves have the same coefficient  $A/T_{\text{coh}}$ , which reveals that the inelastic scattering rate scales with the  $1/T_{\text{coh}}$ . Especially for CeCoIn<sub>5</sub>, it scales with  $1/T^*$  because  $T_{\text{coh}} = T^*$  at  $x \rightarrow 0$  limit.

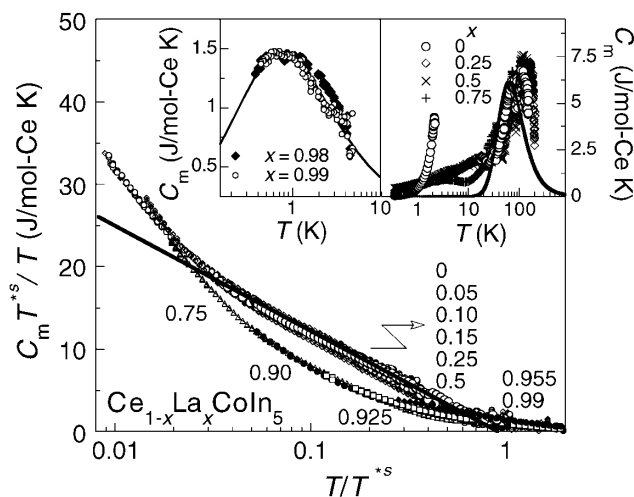


FIG. 3.  $C_m/T$  times  $T^{*s}$  vs  $T/T^{*s}$ . The solid line represents the  $-\ln T$  fit. Left inset:  $T$  dependence of  $C_m$  for  $x = 0.98$  and  $0.99$ . The solid curve is the fit to the  $S = 1/2$  Kondo impurity limit with  $T_K = 1.7$  K. Right inset:  $T$  dependence of  $C_m$ . The solid curve is the fit based on our CEF scheme.

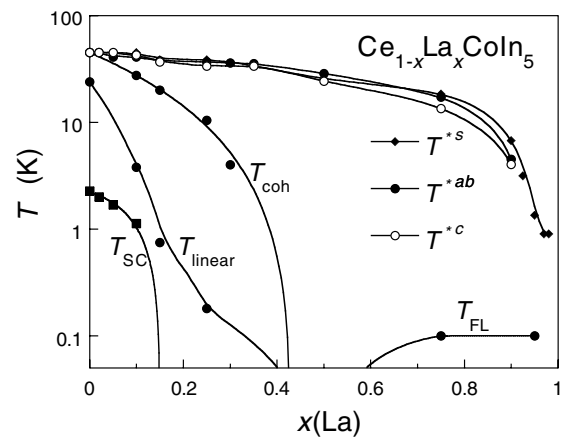


FIG. 4. Energy scale diagram of Ce<sub>1-x</sub>La<sub>x</sub>CoIn<sub>5</sub>.  $T_{\text{sc}}$  is the superconducting transition temperature determined by the onset of the jump observed in  $C_p(T)$ .  $T_{\text{linear}}$  and  $T_{\text{FL}}$  are the temperatures below which the resistivity starts to show  $T$  linear and  $T^2$  dependence.  $T^{*ab}$ ,  $T^{*c}$ , and  $T^{*s}$  are the characteristic temperatures of the  $ab$ -plane and  $c$ -axis susceptibilities, and the specific heat, respectively.

In contrast, the left-hand inset of Fig. 1 displays the  $T^2$  dependence for  $x = 0.75$  and  $0.955$  in the incoherent regime, which becomes evident below the Fermi liquid temperature  $T_{FL} \approx 100$  mK. In the single-impurity limit, according to Nozières and Yamada [16] the  $T^2$  coefficient of the conductivity should be proportional to  $T_K^{-2}$ . Using their formula,  $T_K$  is estimated to be 1.1 K for  $x = 0.955$ . This is consistent with the estimates above.

Non-Fermi-liquid (NFL) behavior is manifested in the  $T$ -linear resistivity and  $-\ln(T/T^*)$  dependence of  $C_m/T$  (Figs. 1 and 3). NFL behavior has been observed in numerous other Ce, Yb, and U alloys and compounds [17] and is frequently attributed to a quantum critical point (QCP) due to the proximity of an AF instability. Especially near a QCP of 2D antiferromagnetism, critical fluctuations are expected to lead to  $\rho \propto T/T^*$  and  $C_m/T \propto -\ln(T/T^*)$  [17,18] as experimentally observed. In this case,  $T^*$  gives the energy scale of the spin fluctuations [17,18].

In addition, several experiments actually point to the 2D AF critical fluctuations. De Haas-van Alphen measurements have shown that  $Ce_{1-x}La_xCoIn_5$  has a strong 2D anisotropy of the Fermi surfaces reflecting its layered structure [10,19]. The resistivity and specific heat under pressure [10,11] and NMR  $1/T_1$  measurements [20] suggest that  $CeCoIn_5$  is close to the QCP of quasi-2D antiferromagnetism. Optical measurements of  $CeCoIn_5$  have revealed the formation of an additional peak below 50 K within the hybridization gap [21], which is attributable to the quasiparticles interacting with AF fluctuations. Notably, their estimate of the fluctuation energy yields the same energy scale (8 meV) as  $T^*$  for  $CeCoIn_5$  (45 K).

Moreover, the decrease of the excess susceptibility  $\Delta\chi$  below  $T^*$  is almost isotropic as shown in Fig. 2, and suggests the development of resonant valence bond-like singlets of  $f$  moments. The  $\Delta\chi(T)$  is well described by the expression  $\Delta\chi(0)[1 - \exp(-0.05T^*/T)]$  with  $\Delta\chi_{ab}(0) \approx -0.038$  emu/mol-Ce and  $\Delta\chi_c(0) \approx -0.052$  emu/mol-Ce. The reduced activation energy  $\Delta = 0.05T^*$  suggests slightly dispersive AF correlations. Interestingly, the  $\Delta$  for  $CeCoIn_5$  gives the same energy scale as the possible pseudogap temperature ( $\approx 3$  K) where the resistivity decrease was observed [11].

These results suggest that spin-liquid formation with the gap  $\Delta$  starts through the screening process, involving the intersite AF correlations with the energy scale  $T^*$ . Furthermore, the qualitative change in the  $T$  dependence of both  $C_m/T$  and  $\rho_m$  around  $x = 0.5$  indicates that a Ce concentration larger than 50% is the criterium not only for coherent transport but also for the intersite coupling leading to a short-range collective mode. This implies that the correlation length is of the order of the lattice constant  $a$  and is rather short compared to what is usually expected for the RKKY interaction.

In summary, we have studied the effects of La dilution on  $CeCoIn_5$ . The scaling laws found in the susceptibility and specific heat reveal a systematic evolution of the

characteristic intersite coupling energy  $T^*$ . Below this temperature, we found a Fermi liquid state in the incoherent impurity regime, while NFL behavior, which scales with  $T^*$ , has been observed in the coherent dense Kondo regime. The latter suggests that the Kondo screening in the lattice is no longer local but rather an intersite effect involving AF spin fluctuations. Given that the ratio of  $T_{sc}$  to the spin fluctuation energy  $T^*$  for  $CeCoIn_5$  ( $\approx 5\%$ ) is of the same order as those for cuprates and other heavy fermion superconductors [18], it is suggestive to associate  $T^*$  with the energy scale leading to the relatively high  $T_{sc}$  of  $CeCoIn_5$ .

The authors acknowledge D. Hall, T. Murphy, and E. Palm for technical support and discussions, and G. Martins, K. Ueda, K. Yamada, and C. M. Varma for comments. This work was performed at the NHMFL, which is supported by NSF Cooperative Agreement No. DMR-9527035 and by the State of Florida. This work is also supported by NSF and DOE through Grants No. DMR-9971348, No. DMR-0105431, and No. DE-FG02-98ER45797. S. N. has been supported by JSPS.

- 
- [1] See, e.g., A. C. Hewson, *The Kondo Problem to Heavy Fermions* (Cambridge University Press, Cambridge, England, 1993).
  - [2] See, e.g., P. Schlottmann, Phys. Rep. **181**, 1 (1989).
  - [3] T. M. Rice and K. Ueda, Phys. Rev. Lett. **55**, 995 (1985).
  - [4] N. Read, D. M. Newns, and S. Doniach, Phys. Rev. B **30**, 3841 (1984); S. Burdin, A. Georges, and D. R. Grempel, Phys. Rev. Lett. **85**, 1048 (2000).
  - [5] H. Tsunetsugu, M. Sigrist, and K. Ueda, Rev. Mod. Phys. **69**, 809 (1997).
  - [6] S. Capponi and F. F. Assaad, Phys. Rev. B **63**, 155114 (2001).
  - [7] See, e.g., Y. Ōnuki *et al.*, J. Phys. Soc. Jpn. **53**, 2734 (1984); N. Sato *et al.*, J. Phys. Soc. Jpn. **54**, 1923 (1985); Y. Ōnuki and T. Komatsubara, J. Magn. Magn. Mater. **63&64**, 281 (1987).
  - [8] C. L. Lin *et al.*, Phys. Rev. Lett. **58**, 1232 (1987).
  - [9] C. Petrovic *et al.*, J. Phys. Condens. Matter **13**, L337 (2001).
  - [10] H. Shishido *et al.*, J. Phys. Soc. Jpn. **71**, 162 (2002).
  - [11] V. A. Sidorov *et al.*, cond-mat/0202251.
  - [12] R. T. Macaluso *et al.* (unpublished).
  - [13] N. J. Curro *et al.*, Phys. Rev. B **64**, 180514(R) (2001); T. Tayama *et al.*, Phys. Rev. B **65**, 180504(R) (2002).
  - [14] A. M. Tsvelick and P. B. Wiegmann, Adv. Phys. **32**, 453 (1983).
  - [15] K. Yamada, K. Yoshida, and K. Hanzawa, Prog. Theor. Phys. **71**, 450 (1984).
  - [16] P. Nozières, J. Low Temp. Phys. **17**, 31 (1974); K. Yamada, Prog. Theor. Phys. **53**, 970 (1975).
  - [17] See, e.g., G. R. Stewart, Rev. Mod. Phys. **73**, 797 (2001).
  - [18] T. Moriya and K. Ueda, Adv. Phys. **49**, 555 (2000).
  - [19] D. Hall *et al.*, Phys. Rev. B **64**, 212508 (2001); D. Hall *et al.* (unpublished).
  - [20] Y. Kohori *et al.*, Phys. Rev. B **64**, 134526 (2001).
  - [21] E. J. Singley *et al.*, Phys. Rev. B **65**, 161101(R) (2002).